# Tropical ocean-atmosphere controls on inter-annual climate variability in the Cretaceous Arctic.

Andrew Davies[1‡], Alan E. S. Kemp[1]*, Heiko Pälike[1]

[1] National Oceanography Centre Southampton, School of Ocean and Earth Science, University of Southampton, Southampton, SO14 3ZH, UK.

*To whom correspondence should be addressed, E-mail: aesk@noc.soton.ac.uk

‡ Present address: Neftex Petroleum Consultants Ltd, Abingdon, OX14 4RY, UK.

Abstract

The first annually resolved sedimentary record from the Cretaceous is used to develop time series of inter-annual and decadal scale climate variability from the Arctic Ocean. Analysis of records spanning 1000 years reveals strong periodicities in the quasi-biennial oscillation and El Niño – Southern Oscillation (ENSO) band as well as a 14 year period, which all closely match periodicities typical of modern high latitude climate variability. This supports the view that an Arctic Ocean free of permanent sea ice would be driven by similar forcing to the present state, implicating tropical ocean atmosphere interaction and demonstrating that stratosphere-troposphere coupling likely played a prominent role in the transmission of Cretaceous equatorial climate forcing to polar latitudes as has recently been established for the modern earth system. On the other hand, the prominent ENSO periodicities in our records argue against the hypothesized link between past warm climates and "permanent El Niño" states.

## 1. Introduction

There is debate as to whether changes in the magnitude and frequency of natural modes of climate variability such as ENSO or the Arctic Oscillation/ North Atlantic Oscillation (AO/ NAO) are forced by anthropogenically driven elevated $CO_2$ and warming or represent natural perturbations of the Earth system [*Corti et al.*, 1999]. For example, will warmer climates result in a more frequent or "permanent" El Niño or favour a positive North Atlantic Oscillation, with milder European winters? In particular, the "permanent" El Niño scenario invoked for the Pliocene and other past and possible future climate states, involving a sustained deeper thermocline and reduced equatorial zonal temperature gradient [*Fedorov et al.*, 2006] has excited particular controversy. The modern Arctic Ocean is regarded as an amplifier of global warming [*Graversen et al.*, 2008] and an early warning system for climate change. Periodicities characteristic of ENSO obtained from records of Arctic sea-ice extent [*Gloersen*, 1995] and other aspects of Arctic climate have motivated observational and modelling studies that have identified mechanisms of transmission of ENSO signals to high latitudes [*Camp and Tung*, 2007; *Ineson and Scaife*, 2009; *Jevrejeva et al.*, 2004]. A key question is whether these presently dominant modes of variability will continue to operate in near-future warmer climates, in an Arctic without permanent sea ice cover? Indeed, there is speculation that ice-free Arctic summers (anticipated within the next 15-50 years; [*Holland et al.*, 2006]) may have significant effects over high and mid-latitude atmospheric circulation patterns and climate variability [*Deser et al.*, 2010; *Seierstad and Bader*, 2009; *Singarayer et al.*, 2006]. Important information about Earth system behaviour in warmer periods is available from former greenhouse episodes such as the Paleogene or Cretaceous. In particular, the Late Cretaceous Arctic Ocean was free of ice in summer with only intermittent sea ice in the winter [*Davies et al.*, 2009]. Records from such ice-free former states may also inform the current discussion about future trends in Arctic variability since there is debate as to the relative importance of snow and ice albedo feedbacks [*Serreze and Francis*,

2006], versus northward atmospheric energy transports in current Arctic warming trends [*Graversen et al.*, 2008; *Screen and Simmonds*, 2010].

**2. Data and Methods**

Short cores from the Alpha Ridge of the Arctic ocean contain shallow buried Late Cretaceous basinal marine sediment comprising laminated diatom ooze with superbly preserved diatoms (Fig.1)[*Davies et al.*, 2009]. The age of the sediment is likely late Campanian (71-76 Myr ago), although an early Maastrichtian age (69-71 Myr ago) cannot be ruled out [*Davies et al.*, 2009]. The preservation of laminae is evidence of water column stratification and bottom water anoxia that was likely promoted by the limited communication to the late Cretaceous world ocean through the shallow Turgay and Fram straits and increasingly restricted Western Interior Seaway (Fig. 1), and substantial river run-off to the Arctic Ocean [*Chin et al.*, 2008] thus enhancing excess precipitation over evaporation. Study of the Canadian CESAR-6 core sediments using Back Scattered Electron Imagery (BSEI) reveals a seasonal succession of two distinct lamina types that represent an annual lamina couplet (Fig. 2) [*Davies et al.*, 2009]. A lamina of diatom resting spores represents flux from the spring bloom and a distinct lamina comprising diatom vegetative cells represents flux from production during the stratified months of the Arctic summer (Fig. 2). The diatom laminae testify to an ice-free summer although the presence of terrigenous material in some of the couplets is evidence of ice rafting by intermittent winter sea ice. The uninterrupted laminated sequences also provide the opportunity for time series analysis of lamina thickness. BSEI was performed on a 58 cm interval from the laminated unit in the CESAR-6 core (core interval 167.5 – 225.5 cm). Measurements of lamina thickness were undertaken on the resting spore lamina; the vegetative cell lamina and of the total annual sediment couplet or 'varve' on two successive intervals respectively of 450 and 507 years duration. Time series were compiled for the two sections counted (Auxiliary Material, Figs. S-1; S-2) and spectral analysis was undertaken using the Singular Spectrum Analysis – Multitaper

Method (SSA-MTM) Toolkit [*Ghil et al.*, 2002] (Fig. 3). To investigate non-stationarity in the time series, wavelet analysis was performed using the wavelet transform software of Torrence and Compo [*Torrence and Compo*, 1998] (Fig. 4).

**3. Results of Spectral Analysis**

Prominent groups of spectral peaks (significant at 99% confidence levels) occur particularly within the quasi-biennial (QB) band, at 4 and 5 years (typical ENSO low frequency (LF) component – sensu *Allan* [2000]) and at the decadal (14 year) range with individual multi-decadal peaks at 25 and 79 years (Fig. 3; Table 1). The QB, ENSO LF and decadal frequencies have all recently been linked to tropical atmosphere and/ or ocean influence on high latitude climate variability [*Jevrejeva et al.*, 2004]. Our QB peaks (dominantly in the range 2.1 – 2.8 years) likely represent a response to the equatorial stratospheric Quasi Biennial Oscillation (QBO), characterised by alternating (average period 2.3 years), easterly and westerly, downward propagating, wind regimes, whose easterly phase stimulates enhanced tropospheric planetary wave activity that disrupts the stratospheric polar vortex [*Baldwin et al.*, 2001]. Due to stratosphere-troposphere coupling, weakening of the polar vortex propagates downward and leads to a weakening and southward displacement of the tropospheric westerlies characterised as a negative AO or NAO state [*Baldwin and Dunkerton*, 2001; *Jevrejeva et al.*, 2004; *Thompson and Wallace*, 2001]. This QBO – polar vortex – AO/ NAO connection is sufficiently robust that the QBO may now be represented in Atmospheric General Circulation Models with well resolved stratospheres to enhance winter forecasting e.g. *Marshall and Scaife* [2009]. In the modern atmosphere-ocean system, *El Niño* interacts with the QBO to increase the rate of downward propagation of the QBO winds resulting in a variation of the (normally 2.3 year) QBO period from 2.1 years (during *El Niño*) to 2.7 years (during *La Niña*) [*Taguchi*, 2010] and this may explain our wider range of QB periods (Table 1). *El Niño* has also recently been shown to affect the polar vortex by similar mechanisms and with similar magnitude to the QBO, with increased

planetary wave activity and disruption of the polar vortex during *El Niño* events [*Camp and Tung*, 2007; *Ineson and Scaife*, 2009] consistent with our 4 and 5 year periods. Studies of phase lag in modern records that link 2.2 – 5.7 year signals in the Arctic (AO) to signals of similar periodicity detected 3 months earlier in El Niño indices and the Southern Oscillation Index (SOI) are also consistent with transmission via planetary waves [*Jevrejeva et al.*, 2004]. It might be argued that our QB periods represent purely an El Niño influence, but the strong recent corroberation for a direct QBO – polar influence together with increasing evidence for an intimate QBO – ENSO inter-relation [*Gaucherel*, 2010; *Taguchi*, 2010] suggest otherwise. For a longer 13.9 year signal from modern records (similar to our 13.5 period), it was found that El Niño indices and the SOI led the Arctic (AO) signal by 1.7 years and this was attributed to interaction between oceanic and atmospheric planetary waves [*Jevrejeva et al.*, 2004].

**4. Discussion**

The ocean-atmosphere forcings described above generated the signals present in the laminae through influence on the amount of diatom production and flux. The extent of production and flux within the spring bloom would be limited by nutrient availability likely governed by the degree of winter mixing and the extent of riverine input. In modern high latitude seas, high NAO indices are associated with a deeper winter mixed layer likely to tap deeper nutrient sources [*Vage et al.*, 2008], so a direct link between NAO/AO variation and export flux from the spring bloom would be expected. As with the modern, a positive Cretaceous NAO/AO would promote a relatively higher intensity in, and a greater degree of northward penetration of storms and thus generate deep mixing as well as generating more runoff. Such a mechanism would also influence nutrient availability later in the growth season therefore influencing production and flux during the summer (as manifest in the thickness of the vegetative cell lamina).

The mechanisms of transmission of equatorial atmosphere-ocean processes to northern high latitudes via planetary waves identified in modern process studies are dependent, in part, on

land ocean configuration and orography. The large land-sea contrasts and extensive mountain ranges in the modern northern hemisphere amplify tropospheric planetary waves, increasing the potential for disruption of the stratospheric polar vortex [*Baldwin et al.*, 2001]. In fact many main elements of the Cretaceous northern hemisphere paleogeography were similar [*Hay et al.*, 1999; *Otto-Bliesner et al.*, 2002]. The Pacific Ocean was larger but with similar overall configuration although it is likely that there was no significant north Pacific marine link with the Arctic Ocean in the latest Cretaceous [*Hay et al.*, 1999]. Planetary waves are also enhanced by topography and there is evidence for an already extensive western north American N-S palaeo-rockies or laramide mountain chain reaching heights of at least 2.5 km during Late Cretaceous [*Dettman and Lohmann*, 2000] (Fig. 1).

Wavelet spectra show all the prominent Cretaceous periodicities to be nonstationary with some showing a striking resemblance to those of modern ENSO time series, in which such nonstationary behaviour is typical [*Torrence and Webster*, 1999] (Fig 4). Observational and modelling studies demonstrate that non-stationarity may also be introduced in the transmission of ENSO signals to high latitudes [*Greatbatch et al.*, 2004]. Such nonstationary behaviour on multi-decadal timescales highlights the difficulties of assigning apparent trends in the behaviour of leading modes of climate variability to current climate warming [*Corti et al.*, 1999]. It further suggests that even in periods of greenhouse warmth there was considerable longer-term change in the dominant frequencies of interannual variability.

Although we present the first evidence for ENSO periodicities in the Cretaceous, time series from laminated lake and evaporite sediments and associated modelling studies have also identified robust ENSO variability from Miocene and Eocene times [*Galeotti et al.*, 2010; *Huber and Caballero*, 2003; *Lenz et al.*, 2010]. In addition to variability in the typical ENSO low frequency band, these records and associated modelling studies indicate quasi-decadal periodicities tied to the tropics [*Garric and Huber*, 2003] similar to our 13.5 year period. This

evidence of dynamic ENSO variability from past "greenhouse" climate states does not lend support to suggestions of a shift to a "permanent El Niño" in past or future warm climate states, at least in the sense of the continual El Niño-like state depicted by *Fedorov et al.* [2006]. Furthermore, the 4 to 5 year periods obtained from Cretaceous as well as Miocene and Eocene records also argue against alternative scenarios for a "permanent El Niño" involving sustained higher frequency El Niño occurrences [*Wunsch*, 2009].

Acknowledgements. The research was funded by a NERC Research Studentship (AD) and NERC Research Grant (AESK). We are grateful to J. Pike and R. Pearce for assistance with diatom and SEM work, to P. Mudie for access to the CESAR-6 core and K. Davis for drafting.

References

Allan, R. J. (2000), ENSO and Climatic Variability in the Past 150 years, in *El Nino and the Southern Oscillation*, edited by H. F. Diaz and M. V., pp. 3-55, C.U.P.

Baldwin, M. P., and T. J. Dunkerton (2001), Stratospheric harbingers of anomalous weather regimes, *Science*, *294*(5542), 581-584.

Baldwin, M. P. et al. (2001), The quasi-biennial oscillation, *Rev. Geophys.*, *39*(2), 179-229.

Camp, C. D., and K. K. Tung (2007), Stratospheric polar warming by ENSO in winter: A statistical study, *Geophys. Res. Lett.*, *34*(4), doi:10.1029/2006GL028521.

Chin, K. et al. (2008), Life in a temperate Polar sea: a unique taphonomic window on the structure of a Late Cretaceous Arctic marine ecosystem, *Proc. Roy. Soc. B-Biol. Sci.*, *275*(1652), 2675-2685.

Corti, S., F. Molteni, and T. N. Palmer (1999), Signature of recent climate change in frequencies of natural atmospheric circulation regimes, *Nature*, *398*(6730), 799-802.

Davies, A., A. E. S. Kemp, and J. Pike (2009), Late Cretaceous seasonal ocean variability from the Arctic, *Nature*, *460*, doi:10.1038/nature08141.

Deser, C., R. Tomas, M. Alexander, and D. Lawrence (2010), The Seasonal Atmospheric Response to Projected Arctic Sea Ice Loss in the Late 21st Century, *J. Clim.*, *23*(2), 333-351.

Dettman, D. L., and K. C. Lohmann (2000), Oxygen isotope evidence for high-altitude snow in the Laramide Rocky Mountains of North America during the Late Cretaceous and Paleogene, *Geology*, *28*(3), 243-246.

Fedorov, A. V. et al., (2006), The Pliocene paradox (mechanisms for a permanent El Nino), *Science*, *312*(5779), 1485-1489.

Galeotti, S., et al. (2010), Evidence for active El Nino Southern Oscillation variability in the Late Miocene greenhouse climate, *Geology*, *38*(5), 419-422.

Garric, G., and M. Huber (2003), Quasi-decadal variability in paleoclimate records: Sunspot cycles or intrinsic oscillations?, *Paleoceanography*, *18*(3), 1068, doi:1010.1029/2002PA000869.

Gaucherel, C. (2010), Analysis of ENSO interannual oscillations using non-stationary quasi-periodic statistics: a study of ENSO memory, *Int. J. Climatol.*, *30*(6), 926-934.

Ghil, M., et al. (2002), Advanced spectral methods for climatic time series, *Rev. Geophys.*, *40*(1), 3.1-3.41, doi:10.1029/2000GR000092.

Gloersen, P. (1995), Modulation of hemispheric sea-ice cover by ENSO events, *Nature*, *373*, 503-506.

Graversen, R. G. et al. (2008), Vertical structure of recent Arctic warming, *Nature*, *451*, 53-56.

Greatbatch, R. J., J. Lu, and K. A. Peterson (2004), Nonstationary impact of ENSO on Euro-Atlantic winter climate, *Geophys. Res. Lett.*, *31*(2), doi. 10.1029/2003GL018542.

Hay, W. W., et al. (1999), Alternative global Cretaceous paleogeography, in *Evolution of the Cretaceous Ocean-Climate System*, edited by E. Barrera and C. C. Johnson, pp. 1-47, Geological Society of America Special Paper 332, Boulder, CO.

Holland, M. M., C. M. Bitz, and B. Tremblay (2006), Future abrupt reductions in the summer Arctic sea ice, *Geophys. Res. Lett.*, *33*(23), doi:10.1029/2006GL028024.

Huber, M., and R. Caballero (2003), Eocene El Niño: Evidence for Robust Tropical Dynamics in the "Hothouse", *Science*, *299*, 877-881.

Ineson, S., and A. A. Scaife (2009), The role of the stratosphere in the European climate response to El Nino, *Nat. Geosci.*, *2*(1), 32-36.

Jevrejeva, S., J. C. Moore, and A. Grinsted (2004), Oceanic and atmospheric transport of multiyear El Nino-Southern Oscillation (ENSO) signatures to the polar regions, *Geophys. Res. Lett.*, *31*(24), L24210, doi:24210.21029/22004GL020871.

Lenz, O. K., V. Wilde, W. Riegel, and F. J. Harms (2010), A 600 k.y. record of El Nino-Southern Oscillation (ENSO): Evidence for persisting teleconnections during the Middle Eocene greenhouse climate of Central Europe, *Geology*, *38*(7), 627-630.

Marshall, A. G., and A. A. Scaife (2009), Impact of the QBO on surface winter climate, *J. Geophys. Res.-Atmos*, *114*, D18110, doi:10.1029/2009JD011737.

Otto-Bliesner, B. L., E. C. Brady, and C. Shields (2002), Late cretaceous ocean: coupled simulations with the national center for atmospheric research climate system model, *J. Geophys. Res.-Atmos*, *107*(D1-D2), doi:10.1029/2001JD000821.

Screen, J. A., and I. Simmonds (2010), The central role of diminishing sea ice in recent Arctic temperature amplification, *Nature*, *464*, 1334-1337.

Seierstad, I. A., and J. Bader (2009), Impact of a projected future Arctic Sea Ice reduction on extratropical storminess and the NAO, *Clim. Dynam*. *33*(7-8), 937-943.

Serreze, M. C., and J. A. Francis (2006), The Arctic amplification debate, *Climatic Change*, *76*(3-4), 241-264.

Singarayer, J. S., J. L. Bamber, and P. J. Valdes (2006), Twenty-first-century climate impacts from a declining Arctic sea ice cover, *J. Clim. 19*(7), 1109-1125.

Taguchi, M. (2010), Observed connection of the stratospheric quasi-biennial oscillation with ENSO in radiosonde data, *J. Geophys. Res.-Atmos*, *115*, D18120, doi.10.1029/2010JD014325.

Thompson, D. W. J., and J. M. Wallace (2001), Regional climate impacts of the Northern Hemisphere annular mode, *Science*, *293*(5527), 85-89.

Torrence, C., and G. P. Compo (1998), A practical guide to wavelet analysis, *Bull. Am. Met. Soc.*, *79*, 61-78.

Torrence, C., and P. J. Webster (1999), Interdecadal changes in the ENSO-monsoon system, *J. Clim.*, *12*, 2679-2690.

Vage, K., R. S. Pickart, G. W. K. Moore, and M. H. Ribergaard (2008), Winter mixed layer development in the central Irminger sea: The effect of strong, intermittent wind events, *J. Phys. Oceanogr.*, *38*(3), 541-565.

Wunsch, C. (2009), A Perpetually Running ENSO in the Pliocene?, *J. Clim.* *22*(12), 3506-3510.

Table 1. Summary of important spectral peaks significant at 99% confidence level. * Peaks of ca. 14 year period at 95% confidence levels were also identified in the K4-1 (14.1 yr) and K8-5 (13.5 yr) vegetative cell time series.

| Period | Total Varve | | Resting spore | | Vegetative | |
|---|---|---|---|---|---|---|
| | K4-1 | K8-5 | K4-1 | K8-5 | K4-1 | K8-5 |
| Quasi-biennial | 2.3 | 2.4 | 2.3 | 2.1 | 2.3 | 2.7 |
| Oscillation | | 2.6 | 2.9 | 2.8 | 2.6 | |
| | | 2.8 | | | (3.1) | |
| 4-5 year | 5.1 | | | 4.1 | | |
| 14 year | | | 13.5* | | | |
| 25 year | | | | | 25.6 | |
| 80 year | | | | | | 79 |

Figure Captions

Figure 1. Main figure shows Alpha Ridge site with late Cretaceous paleogeography. Inset shows modern geography and location of the Alpha Ridge cores: 6 – CESAR-6; 437 – FL-437; 533 – Fl-533 from Davies et al. [2009]. LR – Lomonosov Ridge; MB – Makarov Basin.

Figure 2. **a**. Back Scattered Electron Image (BSEI) of resin-embedded sediment showing darker, higher porosity, diatom vegetative cell laminae, in which the cross sections of diatoms are discernable, interbedded with paler, lower porosity layers composed primarily of diatom resting spores. (scale bar 100 microns). **b** and **c**: Representative topographic SEM images of **b**: diatom resting spores (scale bar 20 microns). **c**: diatom vegetative cells, mainly *Hemiaulus* spp. (scale bar 40 microns); **d**: Schematic of diatom production and resting spore flux from the spring bloom. **e**. Schematic of autumn flux occurring at the breakdown of stratification (the "Fall Dump") of diatom vegetative cells that grew during the summer months.

Figure 3. Multi-taper method (MTM) power spectra of time series from two core intervals, analysed using methods described in Ghil et al. [2002], using settings of 2 for resolution and 3 for the number of tapers. All plots show the calculated power spectra on a logarithmic amplitude scale, together with the auto-regressive order 1 (AR-1) noise background estimation, and 90%, 95% and 99% confidence intervals. Significant peak periods at 99% confidence are labelled. Bandwidth is given in lower left corner. Power spectra are for **a**, Resting spore laminae thickness from interval K4-1 (210.5 – 225 cm depth), **b**, Vegetative laminae thickness from interval K4-1, **c**, Total varve (annual lamina couplet) thickness from interval K4-1. **d**, Resting spore lamina thickness from interval K8-5 (196.5 – 210.5 cm depth), **e**, Vegetative laminae thickness from interval K8-5, **f**, Total varve (annual lamina couplet) thickness from interval K8-5.

Figure 4. Wavelet analysis. **a**, time series of Niño3 SST index from 1871 to 1998 (from Torrence and Compo [1998]) re-sampled to annual resolution to mimic laminae data. **b**, wavelet power spectrum of Niño3 time series. **c**, time series of resting spore lamina thickness from 507 year interval K8-5. **d**, wavelet power spectrum of resting spore lamina thickness from interval K8-5.

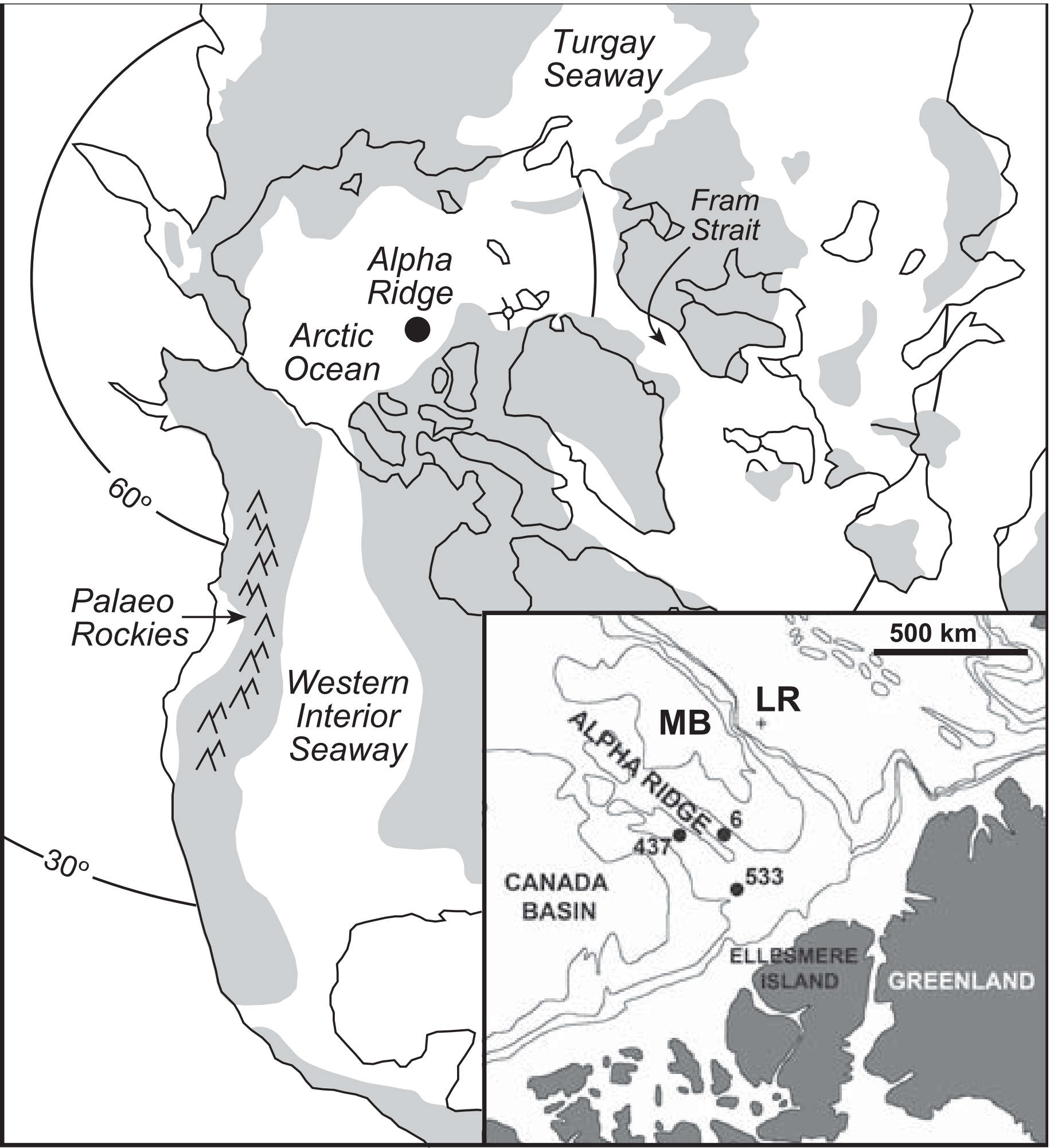
Turgay
Seaway
Fram
Strait
Alpha
Ridge
Arctic
Ocean
60°
Palaeo
Rockies
Western
Interior
Seaway
30°
500 km
LR
MB
ALPHA RIDGE
6
437
533
CANADA
BASIN
ELLESMERE
ISLAND
GREENLAND

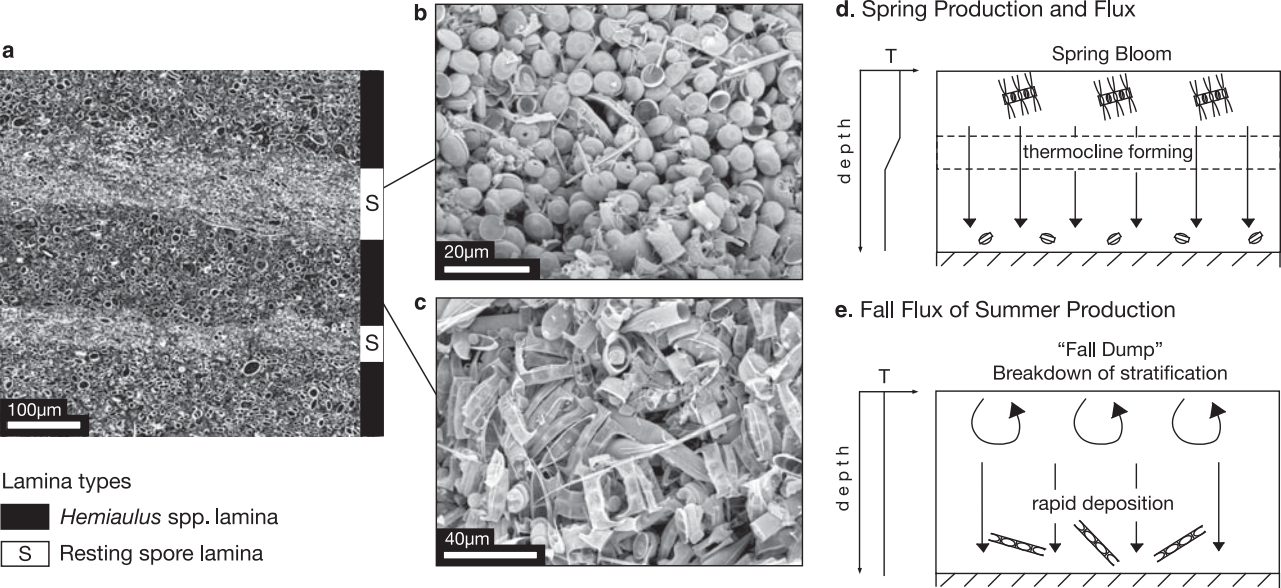
a
b
c
d. Spring Production and Flux
e. Fall Flux of Summer Production
S
S
100µm
20µm
40µm
T
depth
Spring Bloom
thermocline forming
"Fall Dump"
Breakdown of stratification
rapid deposition
Lamina types
Hemiaulus spp. lamina
S
Resting spore lamina

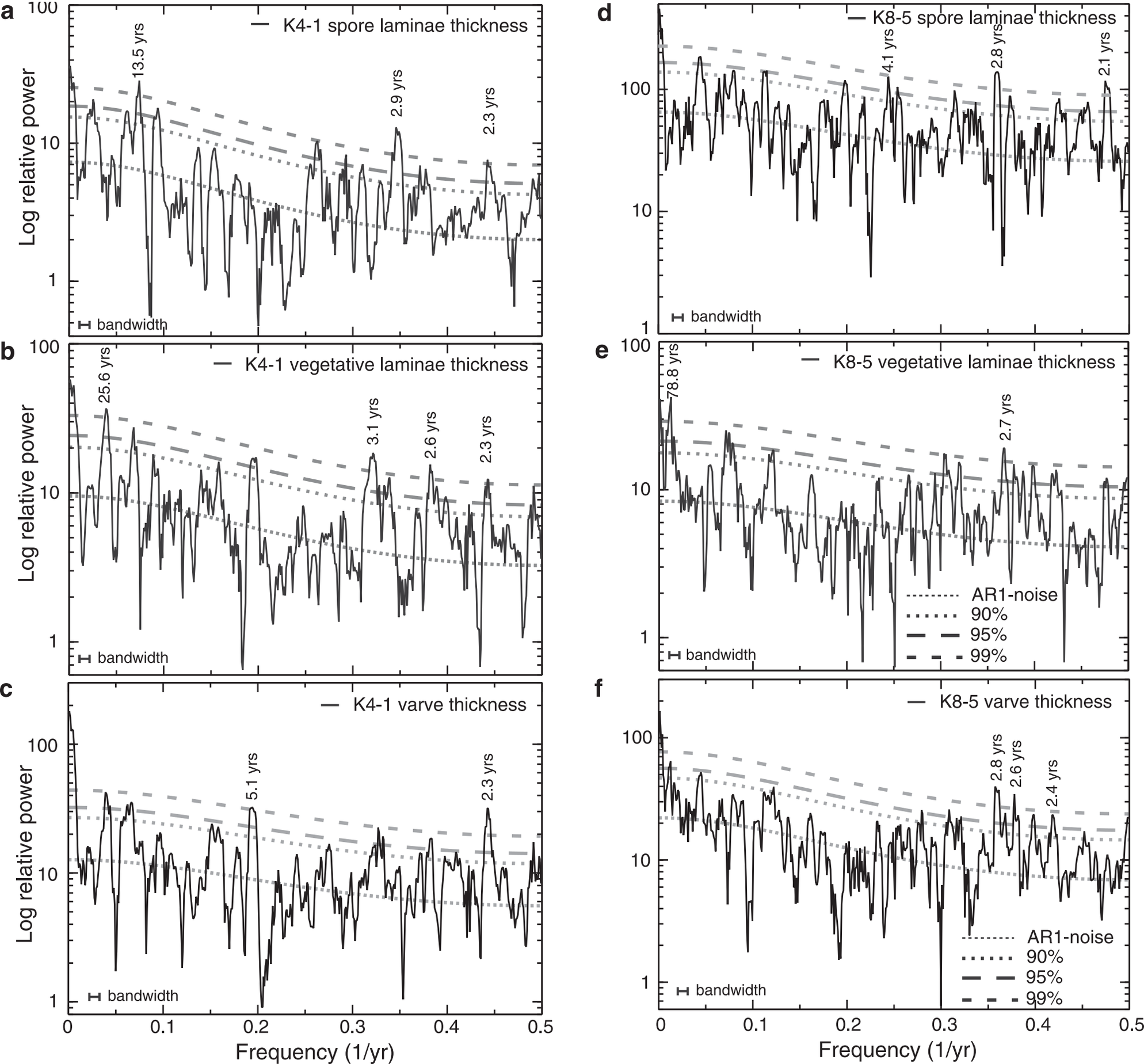
a
K4-1 spore laminae thickness
13.5 yrs
2.9 yrs
2.3 yrs
b
K4-1 vegetative laminae thickness
25.6 yrs
3.1 yrs
2.6 yrs
2.3 yrs
c
K4-1 varve thickness
5.1 yrs
2.3 yrs
d
K8-5 spore laminae thickness
4.1 yrs
2.8 yrs
2.1 yrs
e
K8-5 vegetative laminae thickness
78.8 yrs
2.7 yrs
f
K8-5 varve thickness
2.8 yrs
2.6 yrs
2.4 yrs
Log relative power
bandwidth
AR1-noise
90%
95%
99%
Frequency (1/yr)

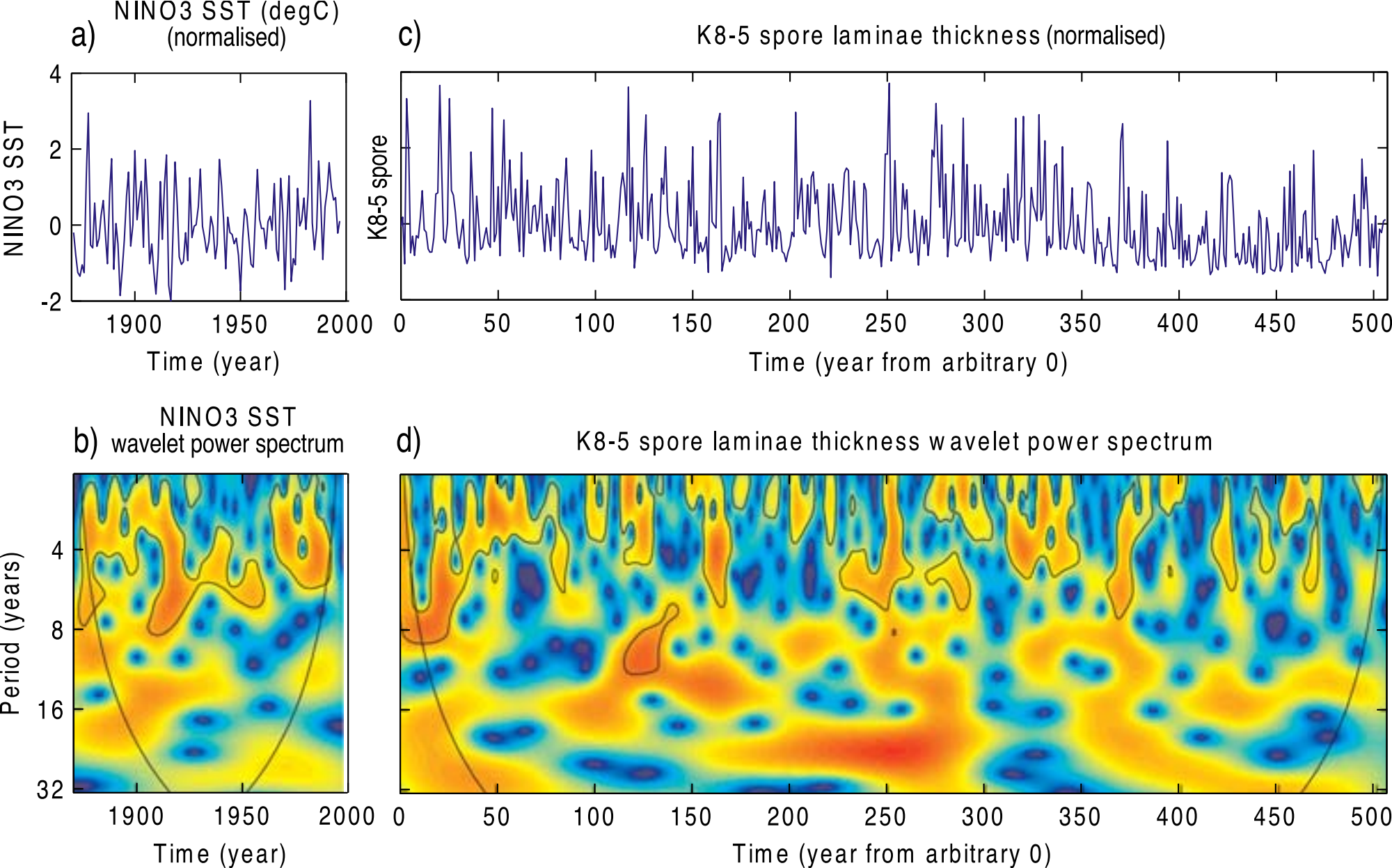
a)
NINO3 SST (degC)
(normalised)
NINO3 SST
4
2
0
-2
1900
1950
2000
Time (year)
c)
K8-5 spore laminae thickness (normalised)
K8-5 spore
0
50
100
150
200
250
300
350
400
450
500
Time (year from arbitrary 0)
b)
NINO3 SST
wavelet power spectrum
Period (years)
4
8
16
32
1900
1950
2000
Time (year)
d)
K8-5 spore laminae thickness wavelet power spectrum
0
50
100
150
200
250
300
350
400
450
500
Time (year from arbitrary 0)